Journal of Scientific & Industrial Research
Vol. 84, July 2025, pp. 790-798
DOI: 10.56042/jsir.v84i7.5474

Green Making of Calcium and Nitrogen Doped Carbon Quantum Dots for Sensing of Pb (II) ion and Anticancer Activity

Sudhaparimala S*, Zaleekha Maryam K A, Usha R & Fairlin Jenitha R

Department of Chemistry, Ethiraj College for Women, University of Madras, Chennai 600 008, Tamil Nadu, India

Received 09 September 2023; revised 22 May 2024; accepted 19 June 2025

Carbon Quantum Dots (CQDs) have garnered significant attention due to their excellent optical properties, making them suitable for various applications. The present study investigates the influence of hetero atoms of Nitrogen, Oxygen, and Calcium on the structural aspects and applications of Carbon Quantum Dots especially in terms of fluorescence sensing and antioxidant properties. A facile and non-toxic microwave-assisted method was used to prepare Nitrogen-doped Carbon Quantum Dots (NCQDs) and Calcium-doped NCQDs (Ca-NCQDs) from the precursor of *Crassostrea virginica* seashell using urea and *Citrus lemon* extract as doping agents, respectively. The impact of doping on the structure-activity relationship and emission (fluorescence) properties of the prepared sample were examined by comparing their microstructure, surface morphology, and elemental composition using analytical tools. Upon evaluating the luminescence and antioxidant activities of NCQDs and Ca-NCQDs, the Calcium doped CQDs showed better intense green fluorescence and enhanced sensing activity of Pb (II) ion while, the Nitrogen-doped CQDs showed more antioxidant and anticancer potential under the given experimental conditions. The results of the study provide great scope for the fabrication of a Pb (II) sensor and anti-cancer agent.

Keywords: Antioxidant, *Crassostrea virginica* seashell, Metal sensor, Microwave method, Tunable fluorescence

Introduction

In recent years, there has been extensive exploration of Carbon-based nanomaterials such as nanodiamonds, fullerenes, Carbon nanotubes, graphene sheets, and fluorescent Carbon quantum dots (CQDs) due to their significant potential for a wide variety of technical applications.[1] The design of novel categories of photoreceptive and sensitive nanoparticles (NPs) from semiconducting and metallic materials has gained considerable importance in biomedical and materials sciences.[2–4] The advanced fluorescence properties of these materials enable their use in diagnostics, therapeutics, imaging, and the sensing of harmful ecological pollutants.[5] However, the extensive use of heavy metals in these advanced materials poses significant limitations, including high toxicity, even at relatively low levels, which may hinder their clinical application.[1,6] This concern has driven the development of Carbon Quantum Dots (CQDs), which offer low toxicity, environmental friendliness, high water solubility, high sensitivity, excellent photostability, selectivity for analytes, low cost, and straightforward synthesis compared to other Carbon-based nanomaterials, along with their tunable fluorescence emissions.

It has been found that upon doping CQDs with Calcium, it forms metal-conjugated CQDs. In Calcium-doped CQDs (Ca-CQDs), the Calcium ion can interact with the surface functional group of C=O on the C-dots, forming a stable structure around the C-dot core, which contributes to a high quantum yield (QY).[7] There are only a few recent research reports available on Calcium-doped Carbon Quantum Dots (CQDs). Chowdhury *et al.,* 2020 – prepared Calcium-modified Carbon dots from polyethylene glycol and synthetic $CaCl_2$.[8] Ren *et al.,* 2021 prepared Calcium capped Carbon quantum dots using urea, citric acid and synthetic $CaCl_2$ via a vacuum heating approach.[7] There is no report to date on the synthesis of Calcium-doped Carbon quantum dots using a natural Calcium source as a precursor viz. Microwave assisted method.

The *Crassostrea virginica* seashell, also known as the Eastern Oyster, plays a key role in maintaining ecological balance. This species is typically found along the Atlantic coast of the United States, the Gulf of Mexico, the West Indies, and the coast of Brazil.[9] Although rare in India, they are found on the

*Author for Correspondence
E-mail: sudha92@gmail.com

seashores of the Gulf of Mannar, especially in Rameshwaram, and were used in this study to prepare Ca-NCQDs. The shell contains Calcium Carbonate in two crystalline forms, aragonite and calcite, as noted by Sudhaparimala *et al*., 2017.[10]

The elemental composition of CQDs from plant sources varies based on the plant species and synthesis method. *Citrus lemon* (L.) Burm, commonly known as the lemon tree, is from the *Rutaceae* family and is native to Asia. It is rich in flavonoids, vitamins, minerals, dietary fibers, essential oils, organic acids, and carotenoids. Lemon and lime juice are rich in citric acid, containing 1.44 and 1.38 g/oz, respectively.[11] Major medicinal properties of *Citrus lemon* (CL) include anti-cancer activity, preventing kidney stones, bringing down a fever and balancing pH.[12] Tadesse *et al.*, 2018 prepared CQDs using *Citrus lemon* extract[13] and Monte-Filho *et al.*, 2019 prepared CQDs using onion and *Citrus lemon* juices.[14] Although there are few reports available on CQDs synthesis using *Citrus lemon* extract, most of them exhibit blue emission, this prompted the idea to prepare CQDs that exhibit green emission, which is safer to DNA when compared to other emissions.

In this work, seven out of twelve principles of Green Chemistry were successfully followed. The microwave pyrolysis method, a well-established bottom-up approach, was used for its rapid synthesis and commercialization benefits. This method is simple, fast, and environmentally friendly, producing Nitrogen-doped Carbon quantum dots (NCQDs) rich in Oxygen-containing groups that serve as coordination sites for metal ions.

To prepare uniform-sized green emissive Calcium-doped NCQDs and study the influence of Calcium on their structure-activity relationship, NCQDs were synthesized with and without Calcium and then compared. Both NCQDs and Ca-NCQDs demonstrated better control over stability and luminescence activities. Depending on their fluorescence emission, these NCQDs and Ca-NCQDs can serve as superior optical sensors for effectively detecting metal ions. The study also explores the radical quenching ability and cell viability against THP-1 cancer cells of the prepared NCQDs and Ca-NCQDs. Thus, exploring simple, energy-efficient processes to prepare Carbon quantum dots and Ca-NCQDs for multi-dimensional applications adds significant research value.

Materials and Methods

Materials

Seashells of *Crassostrea virginica*, particularly found along the seashores of the Gulf of Mannar near Rameshwaram, were used as a source of Calcium. *Citrus lemon* was obtained from the local market in Ayappakkam. The chemicals used for the study of NCQDs and Ca-NCQDs include urea (Nice Chemicals), 99.9% ethanol (Analytical CS reagent), deionized (DI) water, concentrated hydrochloric acid (HCl), 2,2-Diphenyl-1-Picrylhydrazyl (DPPH) (SRL), Lead Nitrate ($Pb(NO_3)_2$) (Nice Chemicals), and Dimethyl sulfoxide (DMSO) (Nice Chemicals).

Microwave-assisted preparation of NCQDs and Ca-NCQDs

The *Citrus lemon* (CL) extract was obtained by removing the seeds and squeezing the *Citrus Lemon*. About 0.5M $CaCl_2$ solution was prepared by dissolving 12.5g *Crassostrea virginica* Seashell powder in Concentrated hydrochloric acid and making it up to 250 mL. The precursors, urea and *Citrus lemon* extract, taken in a 2:1 (w/v) ratio, were stirred for 2 minutes and then heated under controlled conditions using microwave radiation at 140 watts for 10 minutes. The synthesis concluded with the formation of uniform-sized green emissive NCQDs through dehydration and Carbonization processes occurring within the ultrathin spaces of the foam walls.

The Calcium-doped NCQDs (Ca-NCQDs) were also prepared following the above procedure with the addition of $CaCl_2$ (2 mL) to the as-prepared NCQDs from *Crassostrea virginica* seashell under microwave radiation of 140 Watts for 12 mins. Then the dried powder of both NCQDs and Ca-NCQDs was ground well and stored in an air-tight container. The collected two product samples were used for further characterization and application in this present study.

Material Characterization

The functional groups and bonding characteristics of the as-prepared Nitrogen-doped Carbon quantum dots (NCQDs) and Calcium doped NCQDs (Ca-NCQDs) were analyzed using FT-IR (IR Affinity-1, Shimadzu) and UV-Visible absorption spectrometry (UV - Shimadzu 1601). Microstructural analysis was conducted using powder X-ray diffraction (PXRD) with Cu-Kα radiation (PANalytical Xpert Pro) and FT-RAMAN spectroscopy (DST-PURSE). The crystallite size was

calculated using the *Scherrer* equation. Surface morphology was investigated using Field Emission Scanning Electron Microscopy (FE-SEM) (FEI QUANTA), and elemental composition was analyzed with Energy Dispersive X-ray analysis (EDX). Tunable emission properties were studied using a fluorescence spectrophotometer (Cary Eclipse).

Screening the Antioxidant Efficiency of NCQDs and Ca-NCQDs

The DPPH (2,2-diphenyl-1-picrylhydrazyl) quenching assay is a widely used method for evaluating the antioxidant activity of compounds. The assay is based on the reduction of the DPPH radical, a stable free radical, which results in a color change from purple to yellow as it is quenched by antioxidants. The DPPH quenching assay is a straightforward and efficient method to evaluate the antioxidant potential of various substances, making it a standard tool in antioxidant research.[15]

The antioxidant activity of NCQDs and Ca-NCQDs was determined by monitoring the quenching of DPPH. A mixture of 0.025M DPPH with NCQDs and Ca-NCQDs taken individually in a 1:5 (w/v) ratio was incubated at room temperature for 120 minutes. The change in color from deep violet to light yellow was measured by recording the absorbance at 517 nm using a UV-Vis spectrophotometer, indicating a decrease in peak intensity after 120 minutes of reaction.

Sensing of metal toxicity (Pb (II) ion)

The chemical sensing efficiency of the prepared NCQDs and Ca-NCQDs for the metal ion Pb (II) was tested using various concentrations (1µM, 5µM, 10µM) of lead nitrate (Pb $(NO_3)_2$) with a sample concentration of 50 ppm (w/v) of NCQDs and Ca-NCQDs, respectively. The sensing ability of the prepared samples was analyzed by measuring the fluorescence intensity in the presence and absence of the quenching agent.

Anticancer activity -MTT assay method

Cytotoxicity study was carried out through MTT assay. The MTT assay is a colorimetric assay for assessing cell metabolic activity.[16] It is commonly used to determine cytotoxicity, cell viability, and proliferation in cell culture. This study was conducted using the THP-1 cancer cell line (Leukemia) as a model. The viability of THP-1 cells upon exposure to NCQDs and Ca-NCQDs was evaluated. An in vitro MTT assay was utilized to assess the cell viability in response to the functionalized Carbon quantum dots. Human leukemia monocytic cell lines (THP-1) were seeded at a density of 10,000 cells per 200 µL per well in 96-well plates and incubated for one hour. The cells were then treated with a 10 µL compound (5 mg/mL) and incubated for an additional 24 hours. Subsequently, 10 µL of MTT solution, supplemented with 5% feotal bovine serum (FBS), was added, and the cells were incubated for an additional 3 hours. Following this, 100 µL of DMSO was added. Control samples without the test compounds were maintained under the same conditions. The absorbance was quantified at 570 nm.

Results and Discussion

Functional Group Analysis

The FT-IR spectrum of NCQDs and Ca-NCQDs (Fig. 1a) exhibits characteristic vibrations for –OH, -NHCOOH, -C=C-, -C=O, R_2N-N=O, C=N, -$CONH_2$,

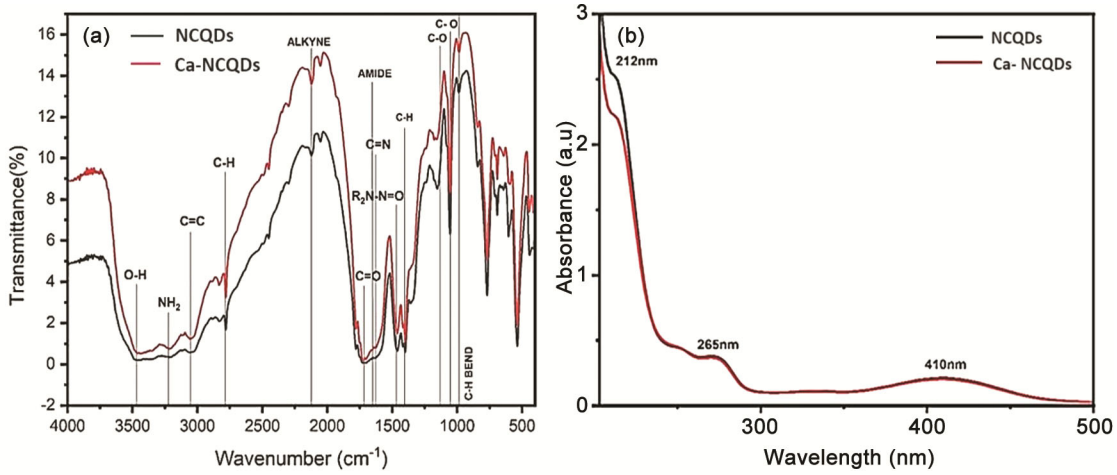

Fig. 1 — (a) FT-IR and (b) UV-Visible spectra of NCQDs and Ca-NCQDs

and C-O at 3468 cm^{-1}, 3223 cm^{-1}, 3052 cm^{-1}, 2127 cm^{-1}, 1722 cm^{-1}, 1466 cm^{-1}, 1649 cm^{-1}, and 1050 cm^{-1}, respectively. The functional groups involving Oxygen, Nitrogen, and Carbon in NCQDs show lower percentage transmittance compared to Ca-NCQDs. The -C=O stretching vibration at 1722 cm^{-1} in NCQDs becomes narrower in Ca-NCQDs, and the amide band at 1649 cm^{-1} becomes more pronounced in Ca-NCQDs due to the presence of Calcium. The enhancement of amide functional groups in the FT-IR spectra of NCQDs doped with Calcium is likely due to a combination of coordination with Calcium ions, changes in surface chemistry, stabilization of amide groups, enhanced hydrogen bonding interactions, and increased sensitivity to FT-IR detection. These effects collectively contribute to the more pronounced and intense amide bands observed in the spectra. This may be due to incomplete conversion of urea into NCQDs by low processing energy. The results confirm the doping of Calcium and its impact on the structure of NCQDs.

The UV-Vis spectrum of NCQDs and Ca-NCQDs exhibits three peaks, as shown in Fig. 1b. A strong peak at 212 nm, 265 nm, and 410 nm is attributed to the π-π* transitions of C=C and n-π* electron transitions of C=O and -C=O-NH_2 groups respectively.[17] This suggests the presence of Carbon atoms bonded with heteroatoms like Oxygen and Nitrogen in the case of NCQDs, and additionally Calcium in the case of Ca-NCQDs. The π-π* transition of Ca-NCQDs at 212 nm is less intense compared to NCQDs, as indicated by the FT-IR data. The reduction in the π-π* transition in the UV spectra of NCQDs upon Calcium doping is likely due to a combination of electronic structure modifications, charge transfer effects, surface passivation, defect introduction, and changes in quantum confinement effects. These factors collectively influence the electronic transitions within the NCQDs, resulting in the observed decrease in π-π* transition intensity.[18] The direct band gaps corresponding to the absorption wavelengths of 212 nm and 410 nm are calculated to be 5.85 eV and 3.02 eV, respectively. There is strong absorption at 265 nm attributed to the π-π* transition, and the corresponding band gap energy is found to be 4.68 eV. These results are consistent with previous reports.[19, 20]

Microstructural Analysis

The PXRD spectrum of NCQDs and Ca-NCQDs (Fig. 2a) exhibited a medium broad peak centered at 2θ = 19.8° and 19.9°, corresponding to the (100) plane, with an FWHM of 0.71 nm and 0.73 nm, respectively, indicating higher amounts of Oxygen-containing functional groups. This is the major characteristic peak of Carbon quantum dots. Another sharp, intense peak centered at 28.1° and 27.9° is observed, consistent with the (002) lattice plane of graphitic Carbon, with an FWHM of 0.97 nm and 1.55 nm for NCQDs and Ca-NCQDs, respectively. The larger FWHM of Ca-NCQDs correlates with the smaller size of the crystallite. The peak intensity of the two peaks in Ca-NCQDs decreased compared to NCQDs upon doping with Calcium. The crystallinity of NCQDs decreased upon Calcium doping, as observed from the larger FWHM value, indicating more defects induced in the structure of Ca-NCQDs. The other less intense peaks are attributed to the incomplete conversion of urea and other micronutrients present in the *Citrus lemon* extract of NCQDs and Ca-NCQDs. The average crystallite size of NCQDs and Ca-NCQDs is 9.97 nm and 9.74 nm,

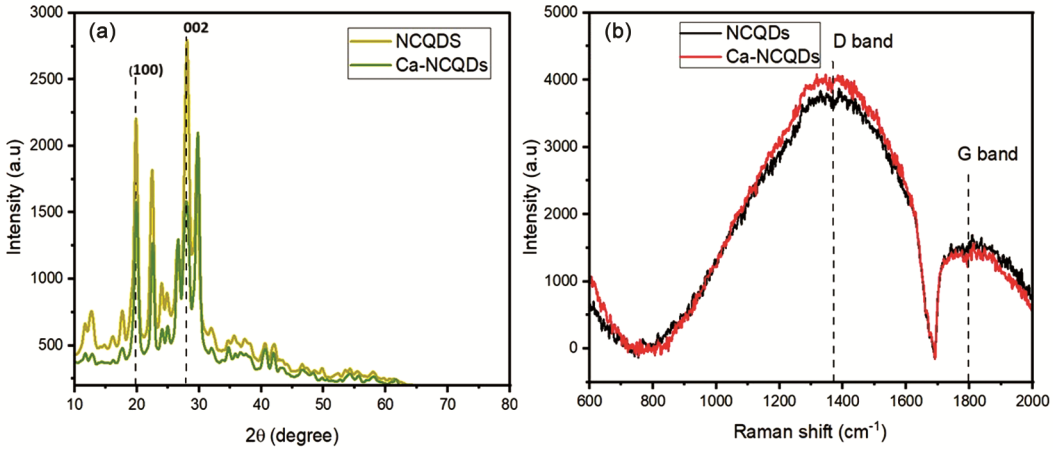

Fig. 2 — (a) PXRD and (b) FT RAMAN spectra of NCQDs and Ca-NCQDs

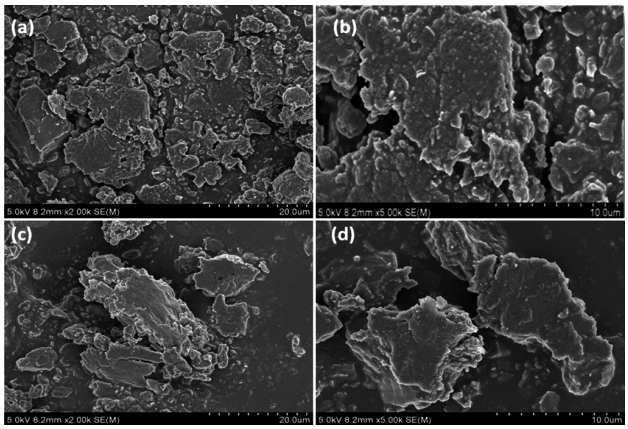

Fig. 3 — FE-SEM images of: (a, b) NCQDs; and (c, d) Ca-NCQDs at different magnifications (20 μm, 10 μm)

respectively, calculated using the *Scherrer* equation. This indicates that the presence of Calcium in NCQDs decreases the size of the Carbon quantum dots, resulting in lower crystallite sites for Ca-NCQDs compared to NCQDs.

The FT RAMAN spectrum of NCQDs and Ca-NCQDs exhibited both the D band at 1332 cm^{-1} and the G band at 1772 cm^{-1} and 1777 cm^{-1}, respectively, as shown in Fig. 2b. The G band corresponds to the E_{2g} vibrational mode of sp^2 Carbon, while the D band arises due to sp^3 Carbon.[19–23] The intensity of the D band (A_{1g} symmetry) in Ca-NCQDs is greater than in NCQDs, likely due to the presence of Calcium in the domain, indicating a large number of defects in the microstructure of Ca-NCQDs. The intensity ratio of the D band to the G band (I_D/I_G) indicates the degree of disorder in the sample, with the ratio being 2.5 for NCQDs and 2.8 for Ca-NCQDs. The increase in the I_D/I_G ratio from NCQDs to Ca-NCQDs signifies more defects and accounts for the highly intense fluorescence of Ca-NCQDs. This correlates well with the PXRD report. The intensity of the G band decreases upon doping with Calcium in the network of NCQDs, suggesting that less sp^2 Carbon exists in the core structure of Ca-NCQDs compared to NCQDs. This finding is well-supported by the UV-visible analysis of Ca-NCQDs.

Surface Property Analysis

The FE-SEM images (Fig. 3) confirm the formation of spherical and quasi-spherical crystallites embedded with Nitrogen and Oxygen in the case of NCQDs, and additionally with Calcium atoms in the case of Ca-NCQDs upon microwave treatment. The size of spherical crystallites is reduced upon doping Calcium into the structure of NCQDs. This morphology of Ca-NCQDs correlates well with the PXRD report. According to the results of PXRD and FT-RAMAN, the defect density in the network of Ca-NCQDs is higher, as observed from the surface of Ca-NCQDs, which shows large aggregates created by the agglomeration of small spherical particles. This correlation is consistent with the reported findings.[7]

The EDX spectra of NCQDs (Fig. 4a) and Ca-NCQDs (Fig. 4b) are shown in Fig. 4. The EDX analysis revealed the elemental presence of Carbon, Oxygen, and Nitrogen in NCQDs, with the additional presence of Calcium in Ca-NCQDs. In Ca-NCQDs, a reduction in the percentage of Oxygen was observed compared to NCQDs. The C/O ratio is relatively higher for Ca-NCQDs compared to NCQDs, indicating a reduction in Oxygen functionality due to the introduction of Calcium. The elemental composition of the prepared NCQDs and Ca-NCQDs along with their respective C/O ratios are presented in Table 1. The Nitrogen content on the surface of Ca-NCQDs was found to be high, likely due to the incomplete conversion of urea into NCQDs. This finding correlates well with the PXRD report and may be attributed to the amide group identified in the FT-IR results.

Evaluation of Antioxidant Properties of NCQDs and Ca-NCQDs

The antioxidant properties of NCQDs and Ca-NCQDs were determined using the DPPH quenching method (Fig. 5).The antioxidant efficiency of NCQDs and Ca-NCQDs was found to be 39.8% and 21.86% respectively. The antioxidant activity of the NCQDs was found to be higher than the Ca-NCQDs. Sudhaparimala *et al.*, reported the anti-oxidant activity of NCQDs (30%) which is lower than the prepared NCQDs but higher than the Ca-NCQDs.[19] In the present study, this may be due to the different experimental conditions. From the results, it is evident that NCQDs have better antioxidant properties than Ca-NCQDs. This may be due to the less Oxygen content present in Ca-NCQDs when compared to NCQDs arising due to the doping of Calcium as identified from EDX spectra.

Photoluminescence (PL) Spectra of NCQDs and Ca-NCQDs

The photoluminescence spectra of NCQDs and Ca-NCQDs Fig. 6(a,b) indicate green emission under UV light qualitatively. It is suggestive of the excitation wavelength-independent tunable emission of the

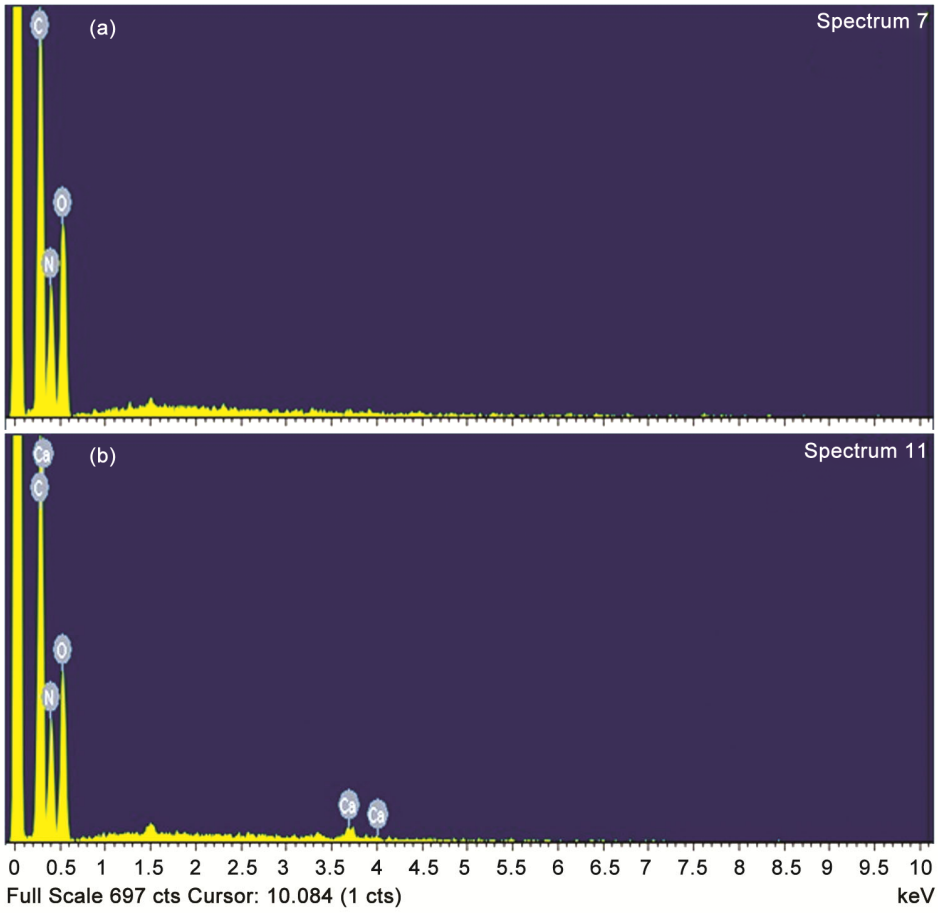

Fig. 4 — EDX spectra of (a) NCQDs and (b) Ca-NCQDs

Table 1 — Comparison of Carbon to Oxygen ratio of NCQDs and Ca-NCQDs

Name of the Elements	NCQDs (Atomic %)	C/O Ratio of NCQDs	Ca-NCQDs (Atomic %)	C/O Ratio of Ca-NCQDs
Carbon	34.66	—	34.68	—
Oxygen	31.66	—	28.50	—
Nitrogen	33.66	1.0948	36.59	1.2168
Calcium	0	—	0.23	—

NCQDs and Ca-NCQDs. The tunable emission spectra of both NCQDs and Ca-NCQDs at different excitation wavelengths (190–280 nm) were observed in the green region.[21–23] The PL confirms the excitation-independent emission in both NCQDs and Ca-NCQDs. The high intense green emission in NCQDs was observed at 526.5 nm whereas Ca-NCQDs showed at 520 nm. The high intense emission peaks indicate the greater recombination of the electron-hole pair of C=N/C=O groups.[18] On comparing both the NCQDs and Ca-NCQDs upon different excitation wavelengths, the Ca-NCQDs have comparatively higher intensity when compared to NCQDs. The Calcium dopant contributes to the formation of sub-defect band gap states interfering with band gap energy of the valance band and conduction band and size of Ca-NCQDs as observed from FT-RAMAN and PXRD reports. The green emission under UV light is comparatively safer than the red and blue emission of nanoparticles from the recently reported by Chowdhury *et al.,* 2020.[8] The result indicates their strong NCQDs and Ca-NCQDs suitability in the bioimaging of healthy and Cancer cells.

Sensing the Metal Toxicity (Pb (II) ion) using NCQDs and Ca-NCQDs

The well-defined emission properties of NCQDs and Ca-NCQDs encouraged further investigation into their potential for chemo-sensing applications, particularly for the detection of heavy and transition

metal ions in aqueous media. The presence of a conjugated π-electron system enhances the ability of NCQDs and Ca-NCQDs to form complexes with a diverse range of metal ions, such as Pb (II) ion.[27] Sudhaparimala *et al.*, 2022 demonstrated the applications of (2D) graphene material for the detection of Cu (II) and Cr (VI) ions.[24] In the present study, zero-dimensional NCQDs are for the detection of Pb(II) ions. The detection of Pb (II) metal ion at different concentrations (1 µM, 5 µM, 10 µM) of lead nitrate (Pb $(NO_3)_2$) using both NCQDs and Ca-NCQDs are given in Fig. 7(a,b). Both the prepared samples were able to sense the Pb(II) ion under the given experimental condition. The lowest detectable limit for both NCQDs and Ca-NCQDs was found to be 1 µM and the sensing efficiency was found to be 17.6% and 23.5% respectively under the given experimental conditions. The quenching rate of the samples was calculated using the *Stern-Volmer* Equation: $\frac{I_0}{I} = 1 + kq[Q]$

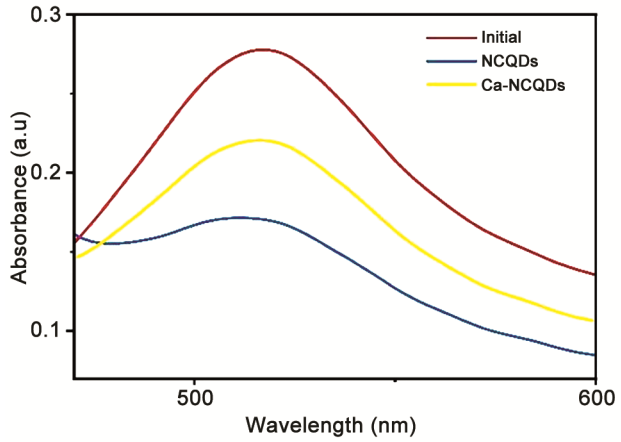

Fig. 5 — DPPH quenching by NCQDs and Ca-NCQDs

where, I_0 and I are fluorescence intensity without and with a quencher, kq – quenching rate, and Q- Concentration of the quencher.

Using the above equation, the spectrofluorimetric quenching reaction rate of NCQDs and Ca-NCQDs with Pb (II) ion was determined. The quenching rate

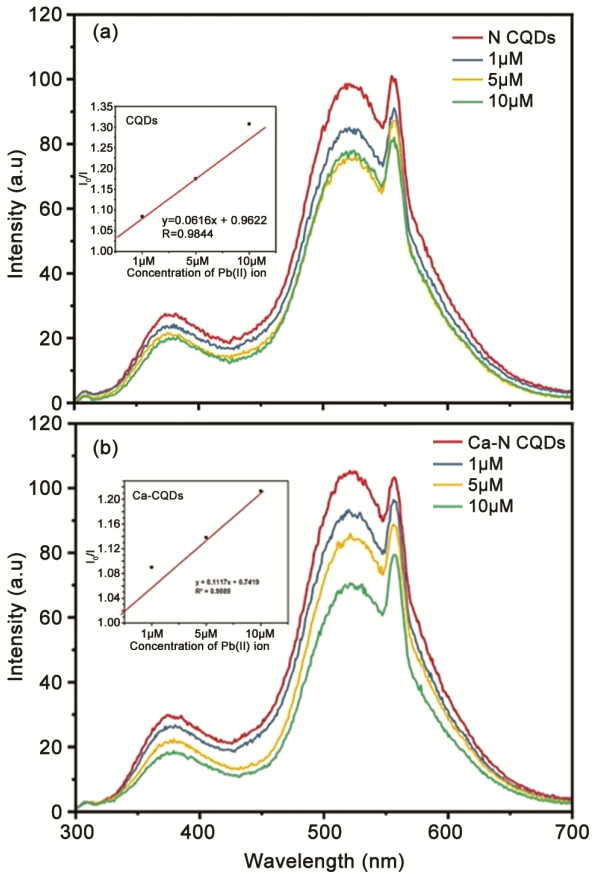

Fig. 7 — Sensing efficiency of the prepared samples with different concentrations of Pb (II) ion and its *Stern Volmer plot* (inset) of (a) NCQDs and (b) Ca-NCQDs

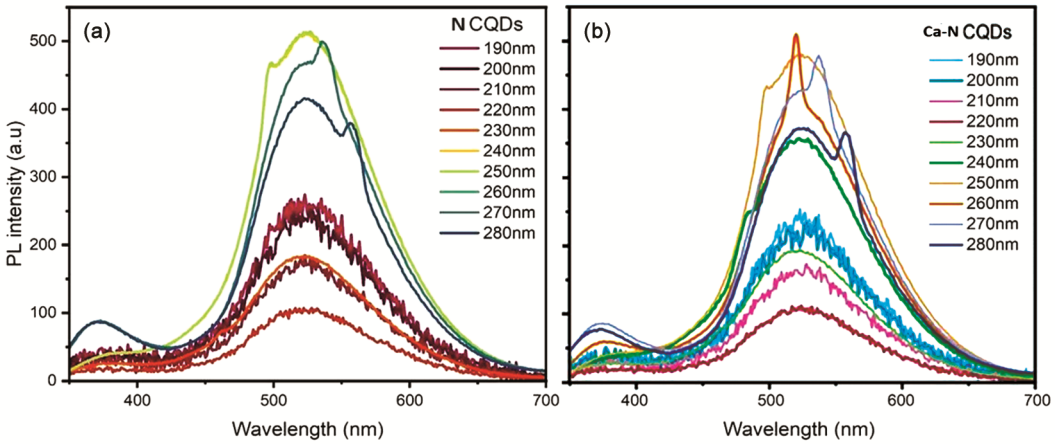

Fig. 6 — Excitation-independent fluorescence spectra of (a) NCQDs and (b) Ca-NCQDs

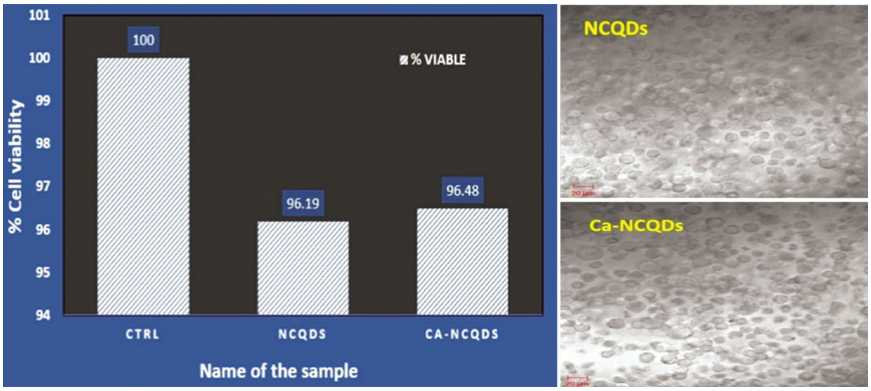

Fig. 8 — Anticancer activity of NCQDs and Ca-NCQDs

for NCQDs was found to be 0.0616 and for Ca-NCQDs it was found to be 0.1117. The *Stern – Volmer* plots of the as-prepared NCQDs and Ca-NCQDs are inserted in the given Fig.7 (a,b). The linear *Stern-Volmer* plot suggests that the sensing of Pb(II) ions follows static quenching. Thus, it can be found that Ca-NCQDs show a higher quenching rate than NCQDs. This may be due to the presence of more defect and functionality due to Nitrogen content as observed from FT-Raman and EDX spectra respectively upon doping of Calcium in NCQDs which eases quenching when compared to NCQDs.

Anticancer activity of NCQDs and Ca-NCQDs

The present study aims to evaluate the cytotoxicity and anticancer activity of NCQDs and Ca-NCQDs against the human monocytic cancer cell line (THP-1) (Fig. 8). THP-1 is a monocyte-like cell line derived from the peripheral blood of a childhood case of acute monocytic leukemia. Leukemia is a group of blood cancers that affect the bone marrow's ability to produce normal blood cells, leading to symptoms such as fatigue, low red blood cell count, and loss of appetite.[25] The toxicity of the prepared NCQDs and Ca-NCQDs was tested against THP-1 cancer cells using the MTT assay method, which is easy to perform, cost-effective, and evaluates the metabolic activity of cells.[28]

The results indicated that both NCQDs and Ca-NCQDs exhibit low toxicity at the tested concentrations compared to the control. Among the prepared samples, NCQDs demonstrated higher anticancer activity than Ca-NCQDs, likely due to the presence of more Reactive Oxygen species (ROS) as observed from the EDX spectra. The ROS generated by NCQDs are involved in the deactivation of cancer cells.[26] The result correlated well with the antioxidant properties of NCQDs. This finding was further confirmed by bioimaging studies. Additional experimental studies are required to further establish the application of NCQDs and Ca-NCQDs in this context.

Conclusions

The study provides a comprehensive report on the production of Carbon quantum dots (CQDs) influenced by Nitrogen and Calcium doping using low-energy method. The experimental conditions were optimized for the preparation of Nitrogen-doped Carbon quantum dots (NCQDs) and Calcium-doped NCQDs (Ca-NCQDs) in a single step. This was achieved using a mixture of seashell (*Crassostrea virginica*) as a Calcium source, Citrus lemon extract, and urea as Carbon and Nitrogen precursors via the microwave method. UV-Visible and FT-IR spectra confirmed the formation of NCQDs and Ca-NCQDs. FT-Raman and PXRD results showed increased defect density and reduced particle size with Calcium doping. Ca-NCQDs exhibited intense green fluorescence and better sensing capability for Pb (II) ions. However, the antioxidant and anticancer potential of Ca-NCQDs was found to be lesser than that of NCQDs. Further studies are required to optimize the synthesis for commercial applications and the fabrication of Carbon quantum dots and their Calcium-doped variants.

Conflicts of Interest

The author(s) declare(s) that there is no conflict of interest regarding the publication of this article.

Acknowledgment

Authors thank the Department of Chemistry and the Instrumentation Centre Ethiraj College for Women, Chennai, India. We thank Dr. M R Ganesh, Assistant Professor, SRM University, kattankulathur, for his contribution to carrying out anticancer analysis.

Funding Source

The author(s) declare(s)that the research work was funded only by the author(s).

References

1 Shi Y L, Wei S & Zhiqiang G, Carbon quantum dots and their applications, *Chem Soc Rev*, **44** (2015) 362–381, https://doi.org/10.1039/C4CS00269E

2 Chaudhary S, Kumar S, Kaur B & Mehta S K, Potential prospects for Carbon dots as a fluorescence sensing probe for metal ions, *RSC Adv*, **6** (2016) 90526, https://doi.org/10.1039/C6RA15691F.

3 Chaudhary S, Umar A & Mehta S K, Surface functionalized selenium nanoparticles for biomedical applications, *J Biomed Nanotech*, **10(10)** (2014) 3004–3042, https://doi.org/10.1166/jbn.2014.1985.

4 Wang B, Song A, Feng L, Ruan H, Li H, Dong S & Hao J, Tunable amphiphilicity and multifunctional applications of ionic-liquid-modified Carbon quantum dots, *ACS Appl Mater Interfaces*, **7(12)** (2015) 6919–6925, https://doi.org/10.1021/acsami.5b00758.

5 Fernando K S, Sahu S, Liu Y, Lewis W K, Guliants E A, Jafariyan A, Wang P, Bunker C E, Sun Y P, Carbon quantum dots and applications in photocatalytic energy conversion, *ACS Appl Mater Interfaces*, **7(16)** (2015) 8363, https://doi.org/10.1021/acsami.5b00448.

6 Geys J, Nemmar A, Verbeken E, Smolders E, Ratoi M, Hoylaerts M F, Nemery B, Hoet P H, Acute toxicity and prothrombotic effects of quantum dots: impact of surface charge, *Environ Health Perspect*, 2008 **116(12)** 1607, https://doi.org/10.1289/ehp.11566.

7 Ren S, Liu B, Han G, Zhao H and Zhang Y, Surface chemistry in Calcium capped Carbon quantum dots, *Nanoscale*, **13(28)** (2021) 12149, https://doi.org/10.1039/ D1NR02763H.

8 Gogoi J, Shishodia S & Chowdhury D, Tunable electrical properties of Carbon dot doped photo-responsive azobenzene–clay nanocomposites, *RSC Adv*, **10(61)** (2020) 37545, https://doi.org/10.1039/d0ra07386e.

9 Willson C, Scotto L, Scarpa J, Volety A, Laramore S & Haunert D, Survey of water quality oyster production and oyster health status in the St. Estuary, *J Shellfish Res*, **24** (2005) 157–165, https://doi.org/10.2983/0730-8000(2005)24[157:SOWQOR]2.0.CO;2.

10 Sudhaparimala S and Usha R, Quality (nanoscale) assessments of Calcium Carbonate present in shells of *Anadara granosa*, and *Crassostreao virginica* marine species located in the coastal part of South India, *Adv Nat Appl Sci*, **11(9)** (2017) 205–212.

11 Penniston K L, Nakada S Y, Holmes R P & Assimos D G, Quantitative assessment of citric acid in lemon juice, lime juice, and commercially-available fruit juice products, *J Endourol*, **22(3)** (2008) 567–570, https://doi.org/10.1089/end.2007.0304.

12 Dev C & Nidhi S R R S, Basketful benefit of citrus limo, *Int Res J Res*, **7(6)** (2016) 1–4, https://doi.org/10.7897/2230-8407.07653.

13 Tadesse A, Rama Devi D, Hagos M, Battu G & Basavaiah K, Facile green synthesis of fluorescent Carbon quantum dots from citrus lemon juice for live cell imaging, *Asian J Nanosci Mater*, **1(1)** (2018) 36–46.

14 Monte-Filho S S, Andrade S I, Lima M B & Araujo M C, Synthesis of highly fluorescent Carbon dots from lemon and onion juices for determination of riboflavin in multivitamin/mineral supplements, *J Pharm Anal*, **9(3)** (2019) 209–216.

15 Usha R and Sudhaparimala S, Enhancing green reduction of graphene oxide by *Nyctanthes arbor-tritis* leaves towards degradation of organic pollutants and tunable fluorescence, *Indian J Environ Prot*, **42(11)** (2022) 1317–1325.

16 Nandishor Jha Geim, Cell Viability and Cytotoxicity: 5 Assays, 2020.

17 Wang Y Q, Wang S S, Zhu J, Wang L, Jiang B H & Zhao W J, Determination of urea content in urea cream by centrifugal partition chromatography, *J Food Drug Anal*, **24(2)** (2016) 399–405, https://doi.org/10.1016/j.jfda.2015.10.005.

18 Zhou D, Jing P, Wang Y, Zhai Y, Li D, Xiong Y, Baranov A V, Qu S & Rogach A L, Carbon dots produced via space-confined vacuum heating: maintaining efficient luminescence in both dispersed and aggregated states, *Nanoscale Horizons*, **4(2)** (2019) 388–395, https://doi.org/10.1039/c8nh00247a.

19 Sudhaparimala S & Fairlin J R, Nitrogen-doped Carbon Quantum Dots from anti-oxidant *Caesalpinia bonducella* for tunable fluorescence and catalytic degradation of dichlorophhenol, *Indian J Appl Res*, **10(6)** (2020) 1–3, https://doi.org/10.36106/ijar.

20 Kung J C, Tseng I T, Chien C S, Lin S H, Wang C C & Shih C J, Microwave-assisted synthesis of negative-charge Carbon dots with potential antibacterial activity against multi-drug resistant bacteria, *RSC Adv*, **10(67)** (2020) 41202, https://doi.org/10.1039/d0ra07106d.

21 Genc R, Alas M O, Harputlu E, Repp S, Kremer N, Castellano M, Colak S G, Ocakoglu K & Erdem E, High-capacitance hybrid supercapacitor based on multi-colored fluorescent Carbon-dots, *Sci Rep*, **7(1)** (2017) 11222, https://doi.org/10.1038/s41598-017-11347-1.

22 Gao J, Zhu M, Huang H, Liu Y & Kang Z, Advances, challenges and promises of Carbon dots, *Inorg Chem Front*, **4(12)** (2017) 1963–1986, https://doi.org/10.1039/C7QI00614D.

23 Bhunia S K, Saha A, Maity A R, Ray S C & Jana N R, Carbon nanoparticle-based fluorescent bioimaging probes, *Sci Rep*, **3(1)** (2013) 1473, https://doi.org/10.1038/ srep01473.

24 Sudhaparimala S & Usha R, Tuning of carbon microspheres and graphene structures with hetero atoms for organic dye degradation and heavy metal remediation-influence of fructose as a precursor, *Nat Environ Pollut Technol*, **21(2)** (2022) 469–480.

25 Daniel Yetman, All About Acute Monocytic Leukemia, 2021.

26 Singh I, Arora R, Dhiman H, Pahwa R, Carbon quantum dots: Synthesis, characterization and biomedical applications, *Turk J Pharm Sci*, **15(2)** (2018) 219–230, https://doi.org/10.4274%2 Ftjps.63497.

27 Jenitha R F & Sudhaparimala S, Microwave conversion of Plantago Psyllium husk into carbon quantum dots for sensing of heavy metals and removal of organic dyes, *Indian J Chem Technol*, **30(6)** (2023) 863–871.

28 Qi H, Qiu L, Zhang X, Yi T, Jing J, Sami R, Alanazi S F, Alqahtani Z, Aljabri M D & Rahman M M, Novel N-doped carbon dots derived from citric acid and urea: fluorescent sensing for determination of metronidazole and cytotoxicity studies, *RSC Adv*, **13(4)** (2023) 2663–2671, https://doi.org/10.1039/D2RA07150A.